UNIVERSITY OF BIRMINGHAM
University of Birmingham Research at Birmingham

Development of a swelling-removal model for the scanning fluid dynamic gauge

Pérez-mohedano, R.; Letzelter, N.; Bakalis, S.

DOI:
10.1016/j.fbp.2014.10.001

License:
Creative Commons: Attribution (CC BY)

Document Version
Publisher's PDF, also known as Version of record

Citation for published version (Harvard):
Pérez-mohedano, R, Letzelter, N & Bakalis, S 2015, 'Development of a swelling-removal model for the scanning fluid dynamic gauge', *Food and Bioproducts Processing*, vol. 93, pp. 269–282.
https://doi.org/10.1016/j.fbp.2014.10.001

Link to publication on Research at Birmingham portal

Publisher Rights Statement:
Eligibility for repository : checked 14/01/2015

General rights
Unless a licence is specified above, all rights (including copyright and moral rights) in this document are retained by the authors and/or the copyright holders. The express permission of the copyright holder must be obtained for any use of this material other than for purposes permitted by law.

•Users may freely distribute the URL that is used to identify this publication.
•Users may download and/or print one copy of the publication from the University of Birmingham research portal for the purpose of private study or non-commercial research.
•User may use extracts from the document in line with the concept of 'fair dealing' under the Copyright, Designs and Patents Act 1988 (?)
•Users may not further distribute the material nor use it for the purposes of commercial gain.

Where a licence is displayed above, please note the terms and conditions of the licence govern your use of this document.

When citing, please reference the published version.

Take down policy
While the University of Birmingham exercises care and attention in making items available there are rare occasions when an item has been uploaded in error or has been deemed to be commercially or otherwise sensitive.

If you believe that this is the case for this document, please contact UBIRA@lists.bham.ac.uk providing details and we will remove access to the work immediately and investigate.

Download date: 05. May. 2023

FOOD AND BIOPRODUCTS PROCESSING XXX (2014) XXX–XXX

Contents lists available at ScienceDirect

Food and Bioproducts Processing

journal homepage: www.elsevier.com/locate/fbp

Development of a swelling-removal model for the scanning fluid dynamic gauge

R. Pérez-Mohedano[a,b,*], N. Letzelter[b], S. Bakalis[a]

[a] Centre for Formulation Engineering, Department of Chemical Engineering, University of Birmingham, Edgbaston, Birmingham B15 2TT, UK

[b] Procter & Gamble Technical Center Ltd., Whitley Road, Longbenton, Newcastle Upon Tyne NE12 9TS, UK

ABSTRACT

A mathematical mechanistic swelling-removal approach has been developed for modelling the cleaning process in dried protein samples using the scanning fluid dynamic gauge (sFDG). The algorithm combines swelling phenomena with removal mechanisms (shear stress removal and soil dissolution). Swelling phenomena were described by applying analytical expressions based on poroelasticity theory. The nonlinear partial differential equation (PDE) describing the thickness swelling ratio was solved numerically, allowing the soil to be divided into theoretical layers. The novelty is presented as the cleaning process is integrated by the elimination of those layers. The model predicts the variation of the soil thickness over time. To describe kinetics of removal, experimental results were considered. Constant removal rates were found after an initial transition period. Removal rates were dependent on the different chemical and physical factors acting: temperature, chemistry concentration (pH, enzyme level), shear stress and frequency of application of shear stress. Soil remaining, total mass or percentage of cleaning over time can also be calculated as outputs. Overall the model has the potential to apply varying cleaning conditions over time and grow to a more theoretical approach in the future by applying enzyme kinetics.

© 2014 The Authors. Published by Elsevier B.V. This is an open access article under the CC BY license (http://creativecommons.org/licenses/by/3.0/).

Keywords: Scanning fluid dynamic gauge; Swelling; Cleaning; Modelling; Enzyme; Cohesive Failure; Theoretical layers

1. Introduction

To remove soft soil deposits off a hard surface it is necessary to overcome the cohesive forces that bind the soil together and the adhesive forces that bind the soil to the substrate. Factors affecting the effectiveness of the removal range from the nature and state of the soil to physical and chemical factors such as flow rate (shear stress applied), concentration of chemicals (pH, enzymes) or temperature (Wilson, 2005).

Fryer and Asteriadou (2009) proposed a classification for cleaning phenomena based on types of soils and mechanisms of removal. Soils were classified based on their physical properties, ranging from *low viscosity fluids* to *cohesive solids*. Cleaning fluids were classified from *water at ambient* to *hot chemicals*. The cleaning mechanism occurring varies depending on the case given: a *fluid mechanic removal* happens when the shear stress imposed by the flow of a fluid over the soil is large enough and no chemicals are needed. However, a *diffusion-reaction removal* involves the presence of chemicals. Different dynamic processes might occur in parallel, involving mass transfer from the bulk of wash solution to the soil, a subsequent diffusion of the actives species, the change of the soil inner properties due to chemical reactions and the increase in moisture content (phase changes). This leads to a weakening of the soil structure that facilitates the cleaning process. Once the soil molecules are disengaged, a reverse mass transfer phenomena occurs. Released particles must travel to the boundary soil-wash solution layer and then be completely removed. The rate limiting stage controls the total removal time.

* *Corresponding author at*: Centre for Formulation Engineering, Department of Chemical Engineering, University of Birmingham, Edgbaston, Birmingham B15 2TT, UK. Tel.: +44 74 111 69186.

E-mail addresses: PMR005@bham.ac.uk, rpmohedano@gmail.com (R. Pérez-Mohedano).

Received 1 July 2014; Received in revised form 30 September 2014; Accepted 1 October 2014

http://dx.doi.org/10.1016/j.fbp.2014.10.001

0960-3085/© 2014 The Authors. Published by Elsevier B.V. This is an open access article under the CC BY license (http://creativecommons.org/licenses/by/3.0/).

Nomenclature

D_{eff}	effective diffusion coefficient
E_a	activation energy
f	frequency function. Step function (0 or 1)
$h(t)$	total sample thickness at time 't'
H	layer thickness in the dry state
J_z	diffusion flux
k	constant incorporating characteristics of macromolecule and penetrant system
k_{ds}	removal rate by soil dissolution
k_{ss}	removal rate by shear stress action
M_t	total sample mass at time 't'
M_0	total sample mass at initial time ($t = 0$)
M_∞	total sample mass at equilibrium ($t = \infty$)
n	diffusional exponent
N	number of polymer chains per unit volume
R^2	coefficient of determination
S	swelling function
SS	shear stress function
SD	soil dissolution function
t	time
T	temperature
x, y, z	Cartesian coordinates
Z	frame at z-axis.

Greek symbols

Δt	time step
Δz	thickness step
λ	stretch in uniaxial direction (thickness at time 't'/dry state thickness)
λ_0	initial stretch – initial swelling ratio (initial thickness/dry state thickness)
λ_∞	stretch at equilibrium – equilibrium swelling ratio (equilibrium thickness/dry state thickness)
Ω	volume of a solvent molecule
χ	Flory–Huggins parameter.

Abbreviations

β-lg	β-lactoglobulin
HDL	high-density lipoproteins
LDL	low-density lipoproteins
NMR	nuclear magnetic resonance
PDE	partial differential equation
sFDG	scanning fluid dynamic gauge
WPI	Whey protein isolate

Particularly, for protein-based soils, three stages can be identified in the cleaning process (Bird and Fryer, 1991):

(1) *Swelling*: An initial swelling process occurs when the soil and the wash solution are put into contact. The diffusion of the liquid containing the active species causes the increase in thickness of the soil.
(2) *Erosion*: Once the active species (e.g. enzymes) have had enough time to act and the increase in moisture content has weakened the soil structure, the removal of the substance starts to occur. A constant removal rate is reached for constant cleaning conditions. Swelling might still be occurring in parallel.
(3) *Decay*: In the final stages of the removal process, adhesive forces become important. For protein-based soils, adhesive forces are typically higher than cohesive forces (Liu et al., 2006). Therefore, higher energy input is required to remove the same soil amount. If cleaning conditions are invariant, then the removal rate is reduced in this latter stage until cleaning is complete.

Modelling cleaning processes over time is a complex task as different transport mechanisms are combined. Not many attempts have been considered so far and semi-empirical approaches are frequent. Dürr and Graßhoff (1999) developed a two-parameter exponential type model as an easy-to-use tool to predict cleaning. A specific time constant was defined as the time required to reach 63.2% of total removal. As a second parameter, a logarithmic-type slope characterising cleaning behaviour was also defined. The model showed high flexibility for describing different cleaning patterns. It was further expanded (Dürr, 2002) to re-appraise the model approach by using a Weibull distribution analysis.

Xin et al. (2004) proposed a mathematical model for the removal of milk protein deposits. Disengagement of protein molecules and subsequent mass transfer to the bulk of the wash solution (boundary layer) were considered to be the rate limiting stages. The initial swelling stage was constrained to occur before a 'reptation time' was reached and no cleaning was observed during this period. The 'reptation time' is linked to the initial time required for the first molecules to disengage. A first-order equation was proposed to characterise the removal rate and a disengagement rate constant introduced. This constant was considered as a function of the volume fraction of the disengaged protein molecules at the soil–solution interface. As the rate limiting stage is the movement of these molecules to the interface and their subsequent detachment, a critical concentration would be reached in this area and a constant removal rate obtained. This agreed with the results seen in experiments. Finally, the decay stage was modelled as a function of the surface area of the remaining film. By integrating the three steps, good correlations (no error given) were obtained with experimental data.

Extensive research has been done to study swelling and dissolution mechanisms on simple protein soil deposits such as β-lactoglobulin (β-lg). Studies performed (Mercadé-Prieto et al., 2007a) showed the presence of a dissolution threshold below which the gel swelled but did not dissolve. This threshold is a function of pH and the volume fraction available inside the protein network. It establishes the limit for the stability of the gels formed. An increase of pH increased the degree of swelling observed. Particularly, significant swelling occurred above pH 10. However, the addition of salts to increase of the ionic strength produced a screening effect between cations from solution and the polymer network. Thus, at a certain level the degree of swelling decreased. Dissolution occurred when pH was high enough (pH threshold) (Mercadé-Prieto et al., 2007b) and a certain swelling ratio was achieved (volume fraction threshold) (Mercadé-Prieto et al., 2009, 2007c). Dissolution rates varied for different alkalinities and solution ionic strengths. A sharp transition in the dissolution rate was found between pH 11 and 12. The disruption of non-covalent intermolecular bonds due to alkali denaturation was established as the main dissolution mechanism. This disengagement was favoured by the repulsion produced due to the increase in the number of charges and the subsequent unfolding of the

Please cite this article in press as: Pérez-Mohedano, R., et al., Development of a swelling-removal model for the scanning fluid dynamic gauge. Food Bioprod Process (2014), http://dx.doi.org/10.1016/j.fbp.2014.10.001

protein structure. Dissolution rates also varied for different protein structures (i.e. length of protein aggregates), which in essence were dependent on the temperature of formation of the gel and the gelation time (Mercadé-Prieto et al., 2006a). For a same pH, higher concentrations of salts produced a repulsion effect due to the presence of more counter ions in the network. The screening effect occurring reduced the degree of swelling and limited the space available. As a consequence, the dissolution rate of the polymer chain was reduced. The disentanglement process (reptation of the polymer chains) was proposed as the dissolution rate limiting removal mechanism. At high pH (pH > 13.3) an anomalous behaviour was also observed (Mercadé-Prieto et al., 2007c, 2006b). A maximum pH for dissolution was found and beyond that point dissolution decreased with the increase of alkalinity. The dissolution rate was not uniform either and dropped over time. To explain that, it was proposed a reduction of the free volume in the gel network due to the high concentration of cations from the alkaline solution (typically NaOH). As the penetration of the alkaline solution occurred, the gel shrunk and the mobility of the protein molecules reduced.

The work also expanded the rate limiting criteria for the dissolution and removal of protein based soils. Three scenarios were established by also considering the effect on removal of an external mechanical action (a flow over the soil sample) (Mercadé-Prieto et al., 2006b). The first case established high temperature, low dissolution pH and a minimum flow. The diffusion of sodium hydroxide into the network or the diffusion of protein molecules into the bulk solution were considered as the two possible limiting mechanisms. Therefore, results suggested that the rate limiting stage was a mass transfer process. The second case assumed high temperatures and high pH. For a low flow, the diffusion of the disengaged molecules into the bulk solution was established as the rate limiting stage. However, for a high flow, the extra mechanical action enhanced the removal rate and the limiting stage was the formation of small aggregates (reaction-controlled). Finally, the third case considered mild conditions of temperature and pH and also a high flow. Due to the high surface shear stress generated, the erosion of the swollen layers occurred and the kinetics of swelling was considered as the limiting mechanism. Similar studies were further performed on slightly more complex protein systems (Whey Protein Isolate/Concentrate) (Saikhwan et al., 2010). Work reported different swelling behaviours depending on the complexity of the protein gels analysed.

In this work, the development of a mechanistic swelling-removal model is proposed. The model was based on experimental data obtained by doing thickness measurements on initially dried egg yolk samples using the scanning fluid dynamic gauge (sFDG) (Gordon et al., 2010a, 2010b). A case study is shown as a guideline to understand decisions made. The identification of the different mechanisms involved in a typical protein-based soil cleaning process was possible: swelling and removal via external application of shear stress or soil dissolution. An equation is then proposed as a mathematical approach to visualise the problem. Different phenomena were initially analysed independently. Uniaxial swelling is described by a non-linear diffusion partial differential equation (Bouklas and Huang, 2012), which allows to discretise the thickness of the sample and to introduce 'theoretical layers'. The equation is based on traditional poroelasticity approach coupling non-linear diffusion and long deformation theories. Both the soil and the solvent are described by four intrinsic properties: N (number of polymer chains per unit volume), χ (Flory–Huggins parameter–solvent/polymer interaction), Ω (Volume of a solvent molecule) and an effective diffusion coefficient (D_{eff}) to characterise the dynamics of the process. Removal was modelled using an empirical approach. The case study shows the frequency of external application of shear as the parameter affecting cleaning time. Swelling and removal mechanisms acting in parallel were decoupled for the same conditions of temperature and pH. Removal rates were calculated from experimental data by subtracting, at same experimental times, thickness change rates for pure swelling tests. Therefore, for specific conditions given, swelling and removal can be modelled independently as a function of the different factors controlled. Finally, the proposed algorithm integrates in parallel swelling and removal mechanisms. The novelty is introduced as the 'theoretical layers' initially defined are removed over time until cleaning is complete.

2. Materials and methods

2.1. *Egg yolk soil samples*

Egg yolk samples were used as the test soil for experimentation. The hydration effects attributed to the amphiphilic properties they possess made them ideal for the purpose of this study. Typical dry composition contains around 33% of proteins and 62.5% of fats with less than 3.5% of minerals and 1% of carbohydrates (Mine and Zhang, 2013). The main plasma phase is formed by high (HDL) and low-density lipoproteins (LDL) that consist on spherical particles where lipid molecules are contained within a layer of protein. Pre-treated egg yolk LDLs at high temperature (above 70 °C) have been reported to form gels due to the aggregation of protein molecules occurring above those temperatures (Denmat et al., 1999; Tsutsui, 1988).

Tiles were obtained from Centre for Testmaterials (product DS-22, C.F.T, BV, Vlaardingen, the Netherlands). They were made by spraying layers of egg yolk over a stainless steel base. Size of the tiles were 120 mm × 100 mm with an approximate egg yolk mass of 1.75 g (±0.04 g) and an estimated initial dry thickness of 68 μm (±14 μm). The initial thickness was estimated by extrapolating the data obtained from sFDG experiments.

To calculate the initial water content, 3 samples were left at 60 °C for 24 h in a vacuum oven (Booth, 2003). The average amount of water lost was 0.11 g (± 0.03 g). This corresponds to a layer thickness of 9 μm.

2.2. *Scanning fluid dynamic gauge*

In Fig. 1 a schematic of the scanning fluid dynamic gauge can be seen.

The technique measures the change in thickness of an immobile soil sample submerged in a wash solution, in situ and in real time (Gordon et al., 2010a, 2010b). A soil sample placed in the upper tank is subjected to the external action of a nozzle through which a gravity-maintained flow is created. The variation in the soil thickness (swelling or removal) as a consequence of its contact with the wash solution and the surface shear stress generated by the nozzle is recorded. The influence of the following factors can be analysed with this technique: soil type, substrate, temperature, chemistry (pH, enzyme level), shear stress and frequency of application of

Please cite this article in press as: Pérez-Mohedano, R., et al., Development of a swelling-removal model for the scanning fluid dynamic gauge. Food Bioprod Process (2014), http://dx.doi.org/10.1016/j.fbp.2014.10.001

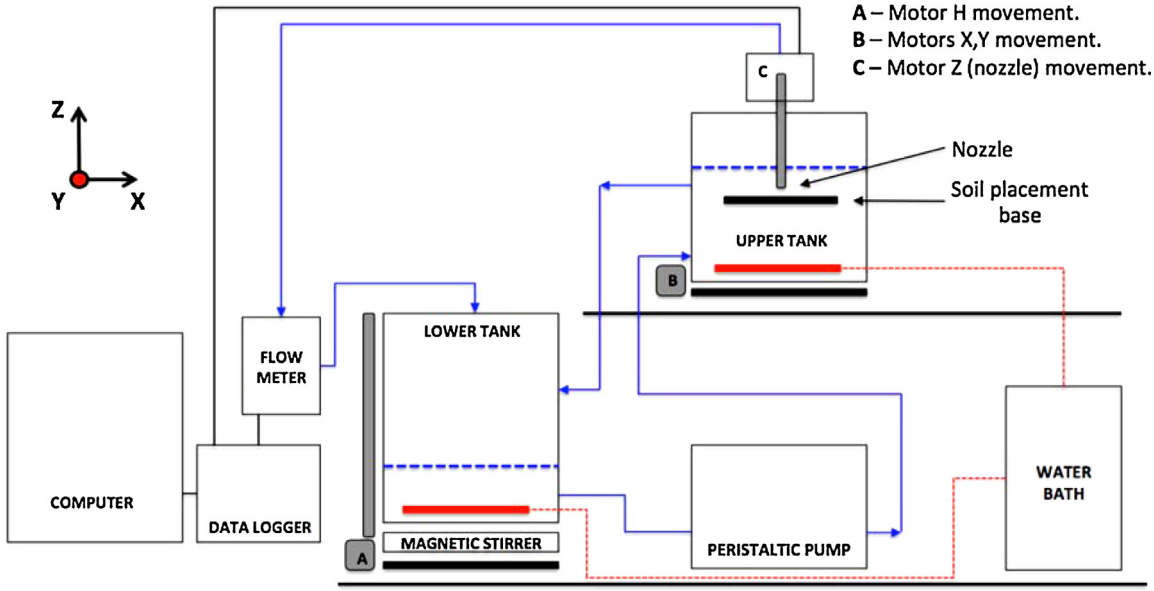

Fig. 1 – Schematic of the scanning fluid dynamic gauge.

the shear stress over a single point as different locations can be tracked. For more specific information, the reader is also referred to (Gordon et al., 2012; Tuladhar et al., 2000, 2002)

2.3. *Case study*

To help the understanding of the model development, experimental conditions seen in Table 1 were considered. These experiments aimed to easily differentiate main cases seen by using the sFDG: no apparent cleaning (test 1), removal by discontinuous (test 2) and continuous (test 3) application of shear stress.

Fixed values of temperature (50 °C), pH (10.5) and shear stress (24 Pa) were established. Two different levels of protease were also examined: none and standard formulation level. Temperature in upper and lower tanks was measured constantly with the aid of waterproof digital thermometers. Buffer solutions were prepared by adding sodium carbonate and pH monitored with a pH meter (product Orion 4 Star™, Thermo Scientific Orion). Shear Stress imposed was estimated at any time by the software controlling the sFDG according to Chew et al. (2005).

Preliminary work demonstrated that at these conditions of temperature and pH no decrease in thickness was observed in the absence of enzymes, suggesting none or insignificant removal. The frequency of application of shear stress over a single location has been considered also here as the factor affecting the total cleaning time. It is defined as the ratio of time the gauging fluid is imposing an external shear stress on a specific location over the total experimental time. A total frequency value of 8.5% was set by tracking 6 different locations per sample and data obtained sequentially at intervals of 1 min. As the nozzle needed time to move from one location to another, the imposition of external shear stress lasted approximately 30 s per location. A frequency value of 100% means that the nozzle is sited over a single location for the duration of the experiment. The above was also expanded in Section 3.3.3 to describe the effect of different temperatures (30 °C, 40 °C and 50 °C) in the removal analysis. These temperatures were selected as representative of the range found in automatic dishwashing cleaning.

3. Results and discussion

3.1. *Typical thickness profiles and data handling*

In Fig. 2A, typical thickness values are shown for a test 1 experiment at three different locations. The graph shows no removal phase (decrease in thickness) and a tendency to the equilibrium, indicating that at the conditions studied no significant removal is detected without the addition of enzymes. Groups of data points were obtained at different times per location. To determine the variability within each sample, a polynomial correlation was established for each of the locations studied. Thickness values were calculated then at fixed times (i.e. every minute). The degree of the polynomial fit was set as the lowest possible to give an accurate fitting ($R^2 > 0.98$), being always 6th order or lower. Typical variability found for a single tile was around 3% of the net thickness. The use of this approach also allowed the comparison of measurements from different repetitions. Data fitted for specific times and for different samples can be further averaged. In Fig. 2B, averaged fitted data from all the locations studied and the triplicates results are shown for the three experimental cases considered. The error was increased up to 6–7% of the net thickness, as the variability from different samples is higher than the variability within a sample. The graph shows a removal stage after an initial net swelling period for cases where protease was present. It also shows a faster cleaning time when a constant application of external shear stress was set (100% frequency). By obtaining thickness values at fixed times, comparison with mathematical models is also simplified.

3.2. *Identification of mechanisms*

In Fig. 3, raw data for a single location in test 2 is shown. Similar plots were obtained for other locations under the same experimental conditions. The figure reveals the three different main mechanisms affecting the thickness change in a soil sample: swelling, removal by shear stress (enzyme-induced disengagement and mechanical action) and removal by soil dissolution (enzyme-induced disengagement and dissolution). As seen in Fig. 2, both types of removal are made possible by the

Please cite this article in press as: Pérez-Mohedano, R., et al., Development of a swelling-removal model for the scanning fluid dynamic gauge. Food Bioprod Process (2014), http://dx.doi.org/10.1016/j.fbp.2014.10.001

Table 1 – Experimental conditions considered for illustration purposes.

Test	Temperature (°C)	pH	Protease level	Shear stress (Pa)	Frequency shear stress (%)
1	50	10.5	None	24	8.5
2	50	10.5	Standard	24	8.5
3	50	10.5	Standard	24	100

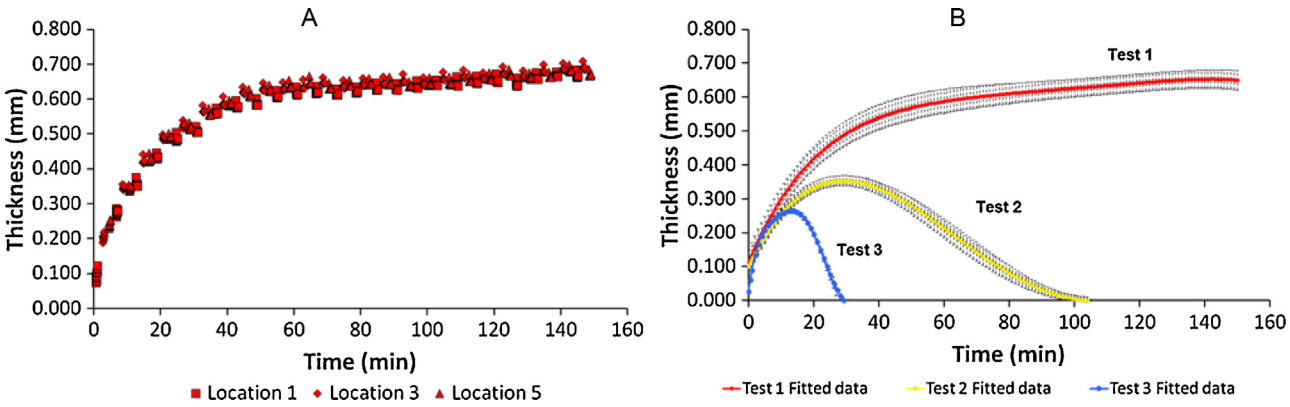

Fig. 2 – A – Raw data values for 3 different locations on the same tile in a single test 1 experiment. B – Averaged fitted experimental results for the three experimental tests considered. Experimental conditions are included in Table 1.

enzymatic action. As there is a lack of bulk fluid movement in these experiments, removal via application of shear stress occurs when the nozzle is positioned on top of a specific location to obtain a height measurement. Removal via soil dissolution occurs when there is no external input of stresses, that is, during the time length where no data is acquired. Soil dissolution mechanism represents the minimum removal rate that can be achieved at the conditions established, with no external disturbances. It corresponds to the mass transfer produced from the soil to the bulk fluid due to chemical action (hydrolysis reactions). The application of an external stress enhances the removal process and soil layers are removed faster. However, the technique does not distinguish the soil disengagement process when an external mechanical input occurs. Molecules to be removed are either already completely disengaged and their transport to the bulk enhanced or the application of the external stress breaks completely the affected areas by the enzymatic action (partially hydrolysed) and produces as well the subsequent transport to the bulk fluid. The origin of disengagement is debatable but has limited effect on modelling results.

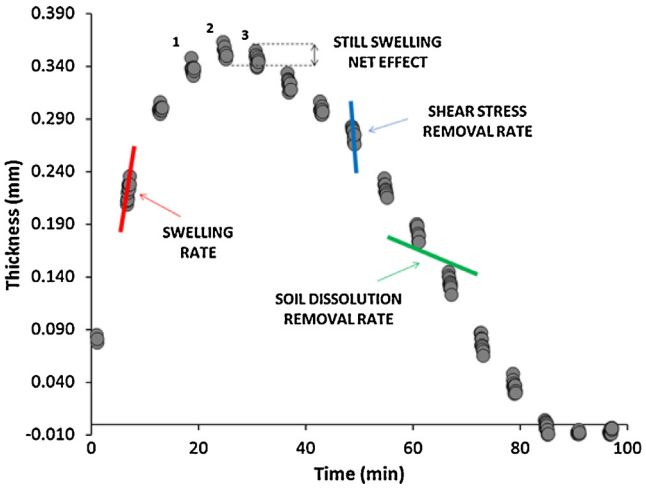

Fig. 3 – Mechanisms identified in a typical protein-based cleaning test in sFDG. Experimental conditions: 50 °C; pH = 10.5; [Protease] = standard formulation level; shear stress = 24 Pa; frequency of application of shear stress = 8.5%. (For interpretation of the references to color in figure legend, the reader is referred to the web version of the article.)

The intensity of the different mechanisms is not constant and varies over time. Around the curve maximum, i.e. at approximately 20–30 min, swelling and removal mechanisms occur at similar rates. Before the maximum thickness (1), the application of an external shear stress produces a net removal effect. The slope of the group of data acquired at that time is negative, indicating a reduction in thickness. Also, as the soil dissolution process is still slower than the swelling rate, an increase in the thickness is seen between consecutive data acquisition periods (1–2). Once the maximum is passed, the swelling rate keeps reducing whilst the dissolution increases. There is still a net increase in thickness at the interval period with no measurements, but that increase is lower than the one seen before the curve maximum (2–3). Later on, both types of removal mechanisms are able to produce a net decrease on soil thickness. The swelling rate is reduced and the sample is weaker and easier to remove.

Similar plots were reported by Gordon et al. (2012), where cleaning studies were also performed on egg yolk stains. The individual modelling of these three mechanisms forms the basics of the proposed algorithm.

3.3. *Algorithm development.*

3.3.1. *Proposed equation*

The above can be summarised using the following equation (Eq. (1)):

$$\frac{dH}{dt} = S - f \cdot SS - (1 - f) \cdot SD \quad (1)$$

where:

- H = thickness
- t = time
- S = swelling function

- SS = shear stress function
- SD = soil dissolution function (based on enzyme effect)
- f = frequency function. Step function (0 or 1).

Thickness variation over time is a function of the different mechanisms involved: swelling and removal via shear stress action or soil dissolution. Each of these mechanisms is modelled individually and integrated together over time. The frequency function is used to account for periods with an external application of shear stress imposed by the sFDG. The external mechanical energy input increases the rate of removal when compared to a pure dissolution process as seen in Fig. 3. Thus, a function that describes when an external shear stress is applied is necessary. This frequency function is a step function taking values of 0 and 1. If an external mechanical action is occurring, the function assigns a value of 1 and the soil dissolution term is cancelled. If cleaning is driven by soil dissolution alone, then its value is 0 and the shear stress term is cancelled. Shear stress function could incorporate some soil dissolution (understood as the complete disengagement of soil elements due to chemical reaction). However, the technique does not completely decouple the removal phenomena as commented previously. For modelling purposes, this approach enables an easier calculation of removal rates.

3.3.2. *Swelling*

To model swelling phenomena, the uniaxial constrained swelling equation (Eqs. (2) and (3)) proposed by Bouklas and Huang (2012) is used. This equation couples mass transport and long deformation theories (Biot, 1941; Flory and Rehner, 1943; Gibbs, 1906). A field of markers (Z) is initially defined across the network structure of the system analysed. As swelling occurs, these markers are displaced thus creating a deformation gradient. Nominal stresses created in the network are antagonised by the chemical potential established between the solvent molecules and the gel. Overall, thermodynamics states that the energy of the system (gel, mechanical deformation load and chemical potential) should never increase. The increase of volume produced in the gel assumes molecular incompressibility, thus is directly related to the absorption of the solvent molecules. The kinetics of the process is based on Fick's second law. An effective diffusion coefficient, D_{eff}, is defined. This parameter is isotropic and independent of the concentration and deformation gradients. The combination of the assumptions made give as a result the following equation for an uniaxial constraint swelling:

$$\lambda_0^2 \frac{\partial \lambda}{\partial t} = D_{eff} \frac{\partial}{\partial Z}\left(\xi(\lambda)\frac{\partial \lambda}{\partial Z}\right) \tag{2}$$

where:

$$\xi(\lambda) = \frac{1}{\lambda_0^2 \lambda^4} - \frac{2\chi(\lambda_0^2\lambda - 1)}{\lambda_0^4 \lambda^5} + N\Omega \frac{(\lambda_0^2\lambda - 1)(\lambda^2 + 1)}{\lambda_0^2 \lambda^4} \tag{3}$$

where:

- D_{eff} = effective diffusion coefficient
- N = effective number of polymer chains per unit volume of the polymer (no. chains/m^3 polymer)
- Z = frame at z-axis
- λ = stretch in uniaxial direction (thickness at time 't'/dry state thickness)
- λ_0 = initial stretch in uniaxial direction (initial thickness/dry state thickness)
- χ = Flory parameter (interaction between the solvent and the polymer)
- Ω = volume per solvent molecule (m^3/solvent molecule).

The total thickness of the sample can be calculated as follows:

$$h(t) = \int_0^H \lambda(z, t)dz \tag{4}$$

where:

- $h(t)$ = total sample thickness at time 't'
- H = layer thickness in the dry state.

Eq. (5) relates the equilibrium-swelling ratio, λ_∞, with N and χ as follows:

$$ln\left(\frac{\lambda_0^2\lambda_\infty - 1}{\lambda_0^2\lambda_\infty}\right) + \frac{1}{\lambda_0^2\lambda_\infty} + \frac{\chi}{\lambda_0^2(\lambda_\infty)^2} + \frac{N\Omega}{\lambda_0^2}\left(\lambda_\infty - \frac{1}{\lambda_\infty}\right) = 0 \tag{5}$$

For a more detailed explanation on the mathematical development, the reader is referred to Hong et al. (2008).

Eq. (2) describes the uniaxial stretch evolution of a soil (hydrogel) that is laterally constrained (or with a negligible lateral stretch variation). The bottom face of the sample is considered to be attached to a rigid substrate ($z = 0$) while the opposite face is freely exposed to the solvent ($z = H$). As hydration occurs, the system swells in one direction (z) while the lateral dimensions remains invariant. The stretch occurring is a function of time and position ($\lambda(z, t)$). The equation is solved using a forward finite difference method. As initial condition it is considered an isotropically swollen state with an initial swelling ratio $\lambda_0(t = 0)$. Boundary conditions establish an instantaneous equilibrium at the top surface (BC1: $\lambda(z = H) = \lambda_\infty$) and a zero flux at the bottom layer (BC2: $J_z(z = 0) = 0$). After a long time ($t \to \infty$) the system evolves to the equilibrium ($\lambda = \lambda_\infty$). It is assumed that the soil surface remains flat during the swelling process, with no formation of wrinkles or creases. The solution of the PDE implies both the discretization of time (Δt) and space (Δz). This allows the introduction of the concept of 'theoretical layers', representing the initial number of layers in which the soil is divided. The concept will be further used to integrate removal mechanisms. To calculate the net thickness variation at a time 't', the stretch profile (λ) obtained needs to be integrated over the layer thickness in the dry state (H) as shown in Eq. (4). From Eq. (5), the equilibrium swelling ratio (λ_∞) shows a dependency on the initial swelling ratio (λ_0) and the intrinsic parameters 'N', 'Ω' and 'χ'. Solutions of the equations given are presented in the appendix section of the paper by Bouklas and Huang (2012).

For the pure swelling case study (test 1), the solution of the system requires an iterative process to fit the unknown parameters. As solvent was water, Ω was estimated to be 3×10^{-29} m^3. The initial stretch (λ_0) and the stretch at equilibrium (λ_∞) were calculated from experimental data. λ_0 was calculated by considering an initial thickness of 68 μm with a water layer thickness of 9 μm, giving $\lambda_0 = 1.15$. To calculate λ_∞ an equilibrium swelling thickness of 605 μm was considered resulting in a value of $\lambda_\infty = 10.3$. Therefore, there were three unknown variables (D_{eff}, χ and N) for the two available equations (Eqs. (2) and (5)). The iterative process started by

Please cite this article in press as: Pérez-Mohedano, R., et al., Development of a swelling-removal model for the scanning fluid dynamic gauge. Food Bioprod Process (2014), http://dx.doi.org/10.1016/j.fbp.2014.10.001

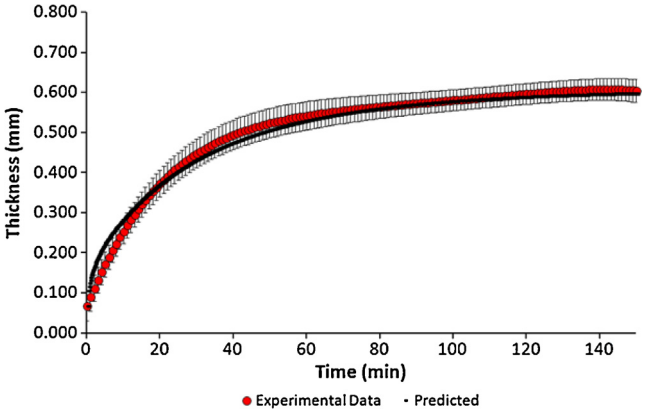

Fig. 4 – Quality of the adjustment for pure swelling experimental data (test 1). Red dots represent averaged fitted experimental data. Black line represents prediction results from model. Experimental conditions: 50 °C; pH = 10.5; [Protease] = None; shear stress = 24 Pa; Frequency of application of shear stress = 8.5%. (For interpretation of the references to color in figure legend, the reader is referred to the web version of the article.)

obtaining stretch profiles ($\lambda(z, t)$) for different combinations of the unknown parameters. Results from Eq. (2) were incorporated to Eq. (4) and thickness profiles over time calculated. These values were compared against experimental averaged fitted results and a coefficient of determination (R^2) calculated. Moreover, Eq. (5) establishes an equilibrium criterion that needs to be fulfilled. A margin of ±0.1 was given to the second term of the equation to account for the experimental error. All χ and N values giving high correlations with experimental results but not complying with the requirement in Eq. (5) were disregarded. A sensitivity analysis showed high sensitivity when predicting D_{eff}. A small change in D_{eff} produced a significant change in R^2. However, lower sensitivity for N and especially χ was seen, thus good predictions were obtained for wider range of values. The iteration showing the highest coefficient of determination (or lower sum of squares error) and satisfying the criterion established by Eq. (5) was the one used as a solution.

In Fig. 4, model predictions results are compared with experimental data. By using the iterative process explained above, the parameters resulting in the best fit were: $D_{eff} = 2.5 \times 10^{-10}$ m^2/s; $\chi = 0.9$; $N = 6 \times 10^{26}$ m^{-3}. 50 theoretical layers were initially defined giving a $\Delta z = 1.22$ μm and a $\Delta t = 0.003$ s. Overall the model compared favourably with the experimental data ($R^2 = 0.98$). A slight over prediction is seen at lower times while predicted values at high times shows great accuracy.

The effective diffusion coefficient (D_{eff}) estimated is closed to those reported by Oztop and McCarthy (2011) for Whey Protein Isolate (WPI) gels ($D_{eff} = 0.79–1.40 \times 10^{-10}$ m^2/s). Their values were estimated by assuming a Fickian diffusion transport model with moving boundaries at pH 7 and 25 °C. Mercadé-Prieto et al. (2008) calculated slightly higher diffusivity values ($D_{eff} = 1.7–1.8 \times 10^{-9}$ m^2/s) for the diffusion of NaOH into β-lactoglobulin. Experimental conditions ranged from 10 °C to 60 °C and a constant NaOH concentration of 0.06 M. Métais and Mariette (2003) reported higher effective diffusion coefficients ($D_{eff} = 0.83–2–14 \times 10^{-9}$ m^2/s) for the penetration of water in fat free and fatty protein concentrates using NMR techniques. Experiments were set between 5 °C and 40 °C and pH 7. Different geometries, experimental conditions and the complexity of the samples analysed could explain the differences observed. The Flory–Huggins parameter estimated was between typical representative values ($\chi = 0–1.2$) (Hong et al., 2009) for high swelling degree gel systems.

The Fickian diffusion hypothesis was tested by applying the semi-empirical equation proposed by Peppas and Sinclair (1983). This equation is valid below 60% of the total equilibrium mass uptake ($M_t/M_\infty \leq 60\%$).

$$\frac{M_t}{M_\infty} = kt^n \quad (6)$$

where:

- k = constant incorporating characteristics of macromolecule and penetrant system
- n = diffusional exponent
- M_t = total sample mass at time 't'
- M_∞ = total sample mass at equilibrium ($t = \infty$)
- t = time.

The value of the diffusional exponent (n) indicates the type of transport occurring. For a thin film, a Case I or Fickian diffusion corresponds to $n = 0.5$ (square root of time). This indicates a solvent diffusion rate much slower than the network relaxation rate. A Case II transport occurs when $n = 1$. In this case, the relaxation of the polymer network limits the diffusion process. A value of 'n' between 0.5 and 1 is termed anomalous transport, which presents intermediate behaviour between Fickian and Case II transport mechanisms.

Gravimetric tests were performed to calculate the diffusional exponent (n). A value of $n = 0.35$ was predicted from results, being slightly lower than for a perfect Fickian diffusion. The effect of an increase in thickness over time, the cross-linking of the gel network and the acidic or alkaline conditions have been reported to influence the diffusional exponent value (Brazel and Peppas, 2000; Peppas and Brannon-Peppas, 1994). The deviation from perfect Fickian transport could explain the initial over prediction given by the swelling model. The complex egg yolk structure could have created an initial extra resistance for the solvent particles to diffuse. Also, the equilibrium occurring at the top layers might be quick, but not instantaneous as assumed theoretically. The rapid thickness increase typically seen at the initial stage could also affect the penetration of the solvent to deeper layers as the travelling distance increases abruptly.

3.3.3. *Removal*

Removal characterisation was done empirically from experimental data. Removal rates in (μm/min) for both shear stress and soil dissolution mechanisms were calculated by determining the different experimental removal slopes (see Fig. 3). Shear stress removal rates were estimated from the groups of thickness data available. For example, for test 2 and as seen in Fig. 3, rates were calculated by linearly fits to those values. The slope (blue line), corresponding to the removal rate at that interval, was assigned to a time value calculated as the average time of the data group analysed. The same procedure was followed to estimate soil dissolution removal rates. The slope from intervals with no data (green line) was calculated and a time value assigned. For cases with a constant application of shear stress (test 3), removal rates were calculated for intervals of 1 min.

Please cite this article in press as: Pérez-Mohedano, R., et al., Development of a swelling-removal model for the scanning fluid dynamic gauge. Food Bioprod Process (2014), http://dx.doi.org/10.1016/j.fbp.2014.10.001

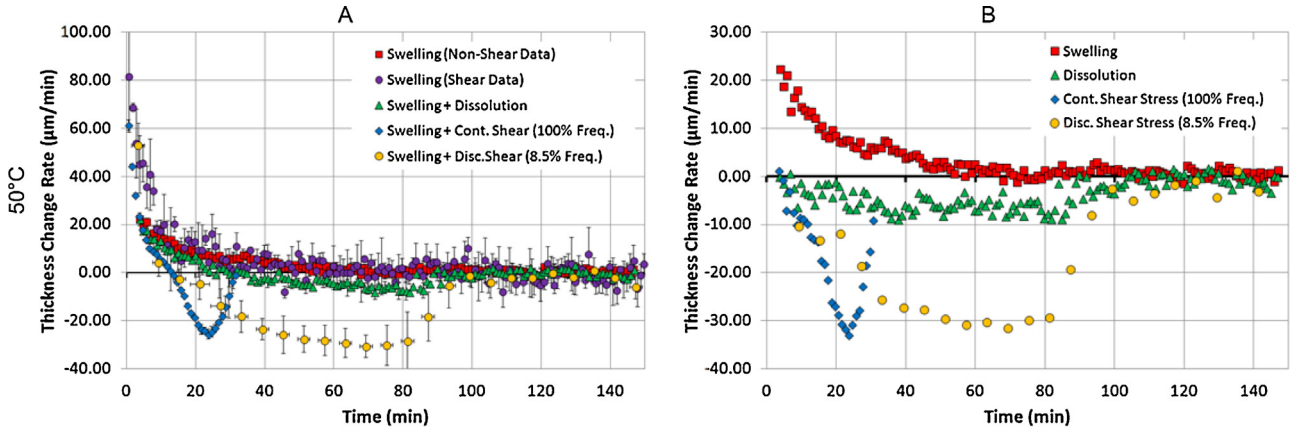

Fig. 5 – Thickness change rate over time for different mechanisms at 50 °C, pH = 10.5 and shear stress = 24 Pa (processed data from test 1–3). A – Mechanisms with swelling phenomena not decoupled. B – Mechanisms with swelling phenomena decoupled. Red squares represent swelling rate data calculated through non-measurement periods for pure swelling test (test 1–[Protease] = none). Purple circles represent swelling rate data calculated through measurement periods for pure swelling test (test 1). Green triangles represent soil dissolution rates obtained from test 2 ([Protease] = standard formulation level). Blue diamonds represent shear stress removal rates with constant application (100% frequency) obtained from test 3 ([Protease] = standard formulation level). Yellow circles represent shear stress removal rates for a discontinuous shear stress application (8.5% frequency) obtained from test 2. (For interpretation of the references to color in figure legend, the reader is referred to the web version of the article.)

Swelling is incorporated as a positive contributor to thickness. In order to decouple swelling and removal mechanisms, swelling rates from test 1 (at the same temperature and pH conditions) were calculated and used as a base line. Positive swelling contributions to thickness were subtracted for each of the interval times considered (i.e. every minute). This assumes a linear relationship between mechanisms. Swelling rates were obtained from either the groups of data points (shear stress applied) or from periods with no data collection (no shear stress applied). The latter showed typically less noise.

In Fig. 5A, the rate of thickness change over time is shown for each of the key mechanisms investigated. The data indicate that swelling had an important positive contribution to the change of the sample height for the first 15 min. At longer times, shear stress resulted in a reduction of the sample height irrespective of the frequency of application (blue and yellow points). A decrease in thickness change rates was also seen as a result of the soil dissolution mechanism (green triangles), but its effect was less strong. The graph also shows higher variability when swelling rates were calculated from the different groups of data points in the experimental readings (purple circles – shear stress applied).

In Fig. 5B, the contribution of swelling to layer thickness was subtracted from removal mechanisms by using the swelling curve (red squares) as a base line. At initial times, removal action showed very little negative effect to the thickness. This negative contribution increased over time and constant removal rates were obtained for soil dissolution (green triangles) and removal via discontinuous application of shear stress (yellow circles) cases, with thickness change rates values of approximately −6 μm/min and −30 μm/min. However, continuous application of shear stress (blue diamonds) did not produce a constant removal rate. The maximum value was reached at approximately 20 min (−32 μm/min) and its subsequent decrease in rate is an indication that cleaning was in its final decay stage. Complete removal was achieved soon after 30 min. The fact that the removal rate was higher between 10 and 30 min for a continuous exposure to shear stress (100%) than for 8.5% frequency suggests a weakening of the soil network at these conditions (50 °C, pH 10.5, 24 Pa). The continuous application of shear is able to produce extra mechanical removal. The graph also illustrates the important difference in removal rates between removal by soil dissolution alone (only enzymatic-induced removal) and shear stress removal (mechanical + enzymatic-induced removal).

The same approach was applied to data collected at 30 °C and 40 °C to determine the effect of lower temperature. Fig. 6 shows the thickness change rate for each of the mechanisms studied. Swelling effect was also subtracted by applying the same approach as for the case at 50 °C. In Fig. 6A and B, removal rates seemed to be constant over time after the initial non-steady period. This includes the case of a constant application of shear stress (blue diamonds). A decrease in the removal rate was also seen after the constant rate period, indicating the final decay stage. Cleaning times were extended as a consequence of the reduction of temperature. In these two cases, higher instantaneous removal rates were obtained when the frequency of application of shear stress was lower (yellow dots versus blue diamonds). This suggests an enzyme reaction rate limiting stage. As the enzyme's function is to help and promote the breakage of peptide bonds (Aehle, 2007), the number of bonds hydrolysed at a certain time is limited. The longer the period without application of shear (lower frequency), the higher the number of bonds affected. As soil dissolution removal (mass transfer process) is slower, when shear stress is reapplied, the amount of soil 'ready to be removed' will be higher. Therefore, higher removal rates will be obtained. For continuous application of shear stress (100% frequency), the instantaneous removal rate achieved will never be higher than a discontinuous application unless the amount of external energy applied (net shear stress value) is able to break mechanically a higher number of inner bonds of the soil network (cohesive failure). An example of this behaviour was commented upon previously for the case of 50 °C. However, the continuous application of shear stress over the soil typically leads to reduced cleaning times as there is no soil dissolution alone.

Please cite this article in press as: Pérez-Mohedano, R., et al., Development of a swelling-removal model for the scanning fluid dynamic gauge. Food Bioprod Process (2014), http://dx.doi.org/10.1016/j.fbp.2014.10.001

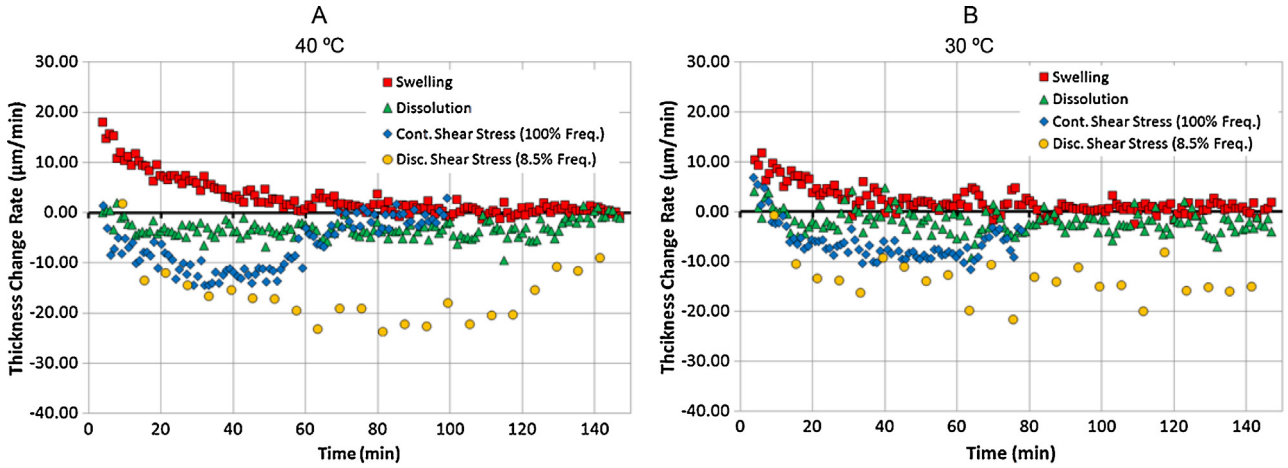

Fig. 6 – Thickness change rate over time for different mechanisms at 40 °C (A) and at 30 °C (B) for pH = 10.5 and shear stress = 24 Pa. Mechanisms with swelling process decoupled. Meaning of the symbols is the same as for Fig. 5.

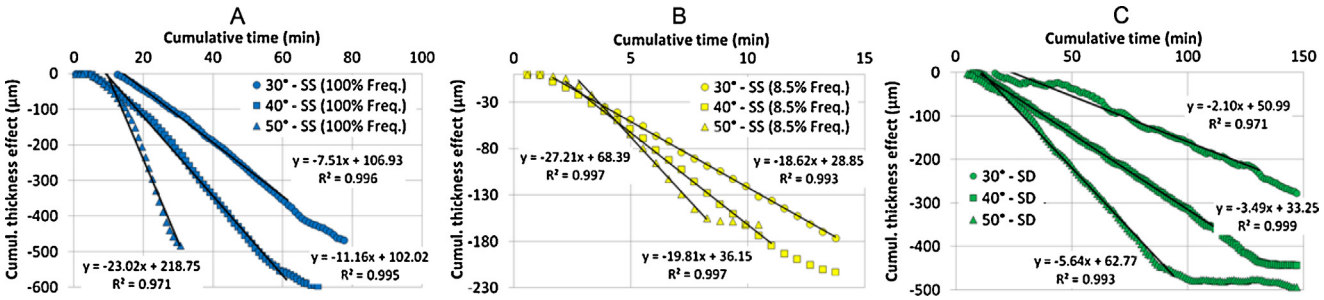

Fig. 7 – Cumulative thickness effect over time at different temperatures and for different cleaning mechanisms. A – Continuous application of shear stress (100% frequency). B – Discontinuous application of shear stress (8.5% frequency). C – soil dissolution. Circles, squares and triangles represent data for 30 °C, 40 °C and 50 °C respectively. Experimental conditions: pH = 10.5; [Protease] = standard formulation level; shear stress = 24 Pa.

Thickness change rates shown previously were integrated over time. In Fig. 7, the resulting cumulative effect on thickness over the cumulative integrated time is seen for cases of continuous and discontinuous application of shear stress and for soil dissolution mechanisms. Their different effects are also seen for the three different temperatures previously shown (30 °C, 40 °C and 50 °C). Given the linear tendency observed, the data were fitted to a linear correlation. The gradient was an estimate of a constant removal rate for each of the cases considered. A lag time was also calculated as the initial time with no cleaning. Its value was established as the intercept on the time axis (*x*-axis).

In Fig. 8, estimated removal rates are compared for all mechanisms at the temperatures studied. Higher removal rates were observed for a discontinuous application of shear as consequence of the enzyme reaction rate limiting stage. As temperature increased, removal rates increased regardless of the mechanism taking place. The energy requirement needed to break cohesively the soil network was reduced as temperature increased. At 50 °C, an approximation between rates from frequencies of 100% and 8.5% is seen. The hypothesis suggests an extra mechanical breakage of some inner bonds of the soil network when a continuous shear is applied. The soil dissolution values represent the maximum amount of soil removed if cleaning occurs without any external action.

An Arrhenius analysis was performed on the soil dissolution data as described by Mercadé-Prieto and Chen (2006). This gave an activation energy (E_a) of approximately 4.8 kJ/mol, slightly lower but in the same order of magnitude than for a non-catalysed breakage of peptide bonds (8–10 kJ/mol) (Martin, 1998). This enhances the hypothesis already given of a reaction rate limiting stage. Despite only three points were analysed (three temperatures considered), a linear correlation was seen when representing removal rates (ln SD) as a function of temperature (1/T). The coefficient of determination estimated was high ($R^2 = 0.999$). This suggests that the

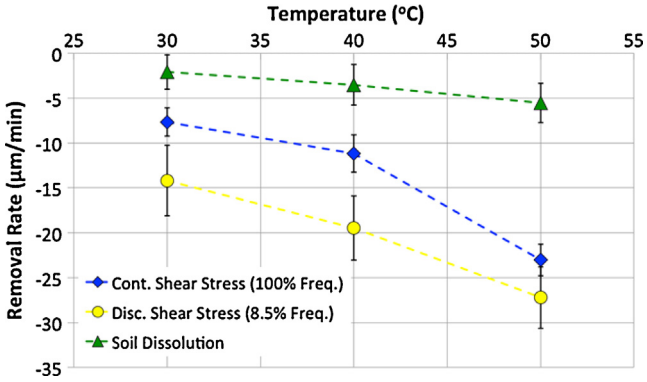

Fig. 8 – Constant removal rates calculated for different mechanisms at different temperatures. Green triangles represent removal rates for soil dissolution. Blue diamonds and yellow dots represent removal rates for a continuous (100% frequency) and discontinuous (8.5% frequency) application of shear stress over the soil. Experimental conditions: pH = 10.5; [Protease] = standard formulation level; shear stress = 24 Pa. (For interpretation of the references to color in figure legend, the reader is referred to the web version of the article.)

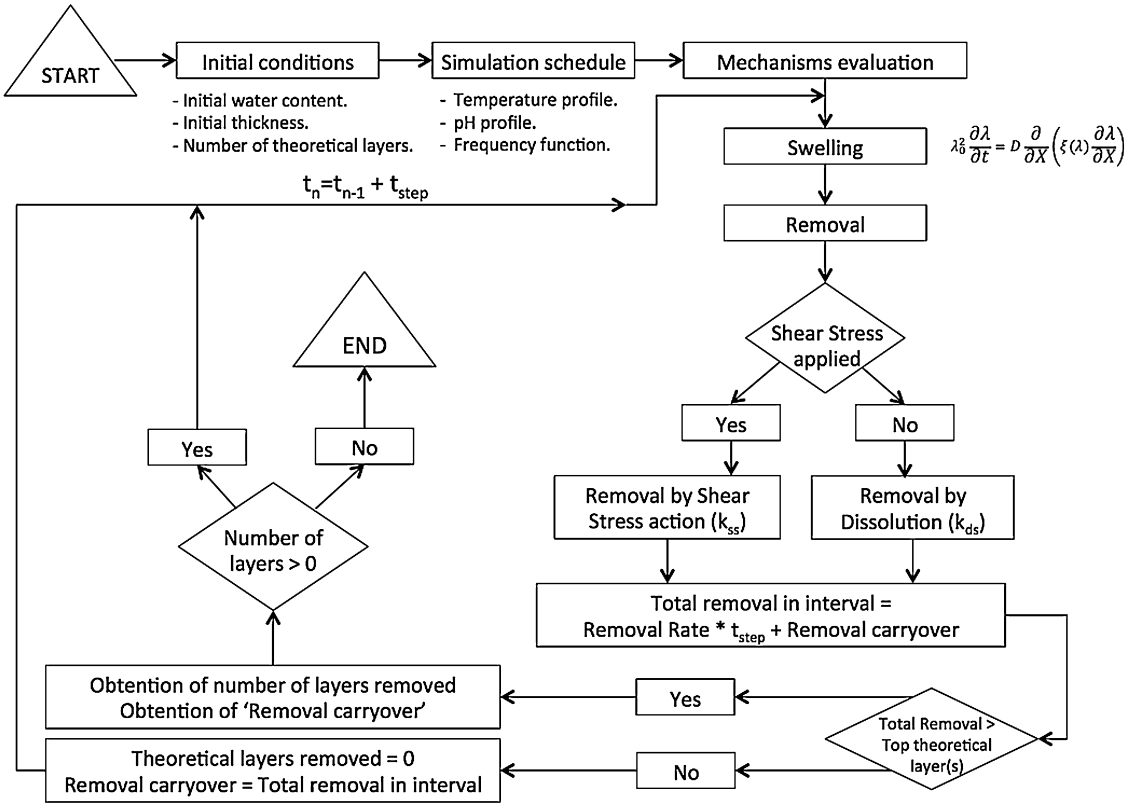

Fig. 9 – Schematic of the algorithm developed.

rate limiting stage is the same independently of temperature. A deeper analysis on this phenomenon will require the study of the dissolution behaviour at different pH, enzyme levels or sample processing conditions.

The empirical approach followed in this section was used to calculate removal rates. Different cleaning mechanisms can be modelled statistically as a function of the parameters controlled. The examples given have shown the effect of temperature and frequency of application of shear stress. Two phases of the cleaning process are distinguished: an initial stage with no removal defined by a lag time and a subsequent constant removal phase. To compensate for the sudden increase in removal rates that this approach would produce, a transition period was also defined. A linear increase in the removal rate was established after the initial lag time for an extra half of the lag time estimated. The use of this transition period is used to provide smoother simulated curves around the curve maximum. An opportunity for further development is possible. The application of a stronger theoretical background to characterise enzyme kinetics (i.e. Michaelis–Menten approach) would lead to a removal model that would be less empirical.

Concerns about a change over time (decrease) of the *N* parameter (the effective number of polymer chains per unit volume of the polymer) can also arise when analysing the definition of the parameter in detail. Hydrolysis reactions breaking protein network bonds reduce the number of crosslinks and long chains. Therefore, the value of *N* reduces. However, removal occurs from top to bottom layers and experimental data suggests an enzyme reaction rate limiting stage. This indicates that only top layers are affected by the enzymatic action at a given time. Those layers are removed as soon as an external mechanical action is applied or through a dissolution process. Deeper layers remain unreacted and therefore with the same 'N' value initially established. Thus, the integrated swelling process can still be applied without any changes over time. For further developments, the decrease of *N* in top layers could be used as limit criteria to establish the point from which removal is going to occur.

3.3.4. *Developed algorithm*

A computer routine developed in MATLAB™ allowed the integration of the different mechanisms studied. In Fig. 9, a schematic of the algorithm used is shown:

Initially, starting conditions for the different experimental variables (temperature, pH, [Enzyme], shear stress, frequency of shear stress) and their profiles along the simulation must be established. These factors are linked (if previously modelled) with the parameters defining both the swelling and removal mechanisms. The initial thickness of the sample is discretised into a number of *theoretical layers* and a *time step* established to comply with the convergence in the solution of the swelling non-linear partial differential equation (PDE). The model evaluates and combines each of the mechanisms (swelling and removal) for every time step. Cleaning happens either by shear stress removal or soil dissolution depending on whether some external mechanical input is applied or not (frequency function). The net removal rate at any stage is given by the approach explained in Section 3.3.3. The integration over the time step gives a net thickness swelling/removal value. To compute for swelling and removal in parallel, the algorithm developed introduces a novel consideration: a deletion of theoretical layers occurs when the integrated rate of removal over a time step is higher than the thickness of the top layer(s) considered. A 'removal carryover' is also calculated as the difference between the net removal in that step time and the net thickness of the layers removed (if there is any layer removed). The routine keeps on calculating the thickness profile over time until no theoretical layers remain (Fig. 10).

Please cite this article in press as: Pérez-Mohedano, R., et al., Development of a swelling-removal model for the scanning fluid dynamic gauge. Food Bioprod Process (2014), http://dx.doi.org/10.1016/j.fbp.2014.10.001

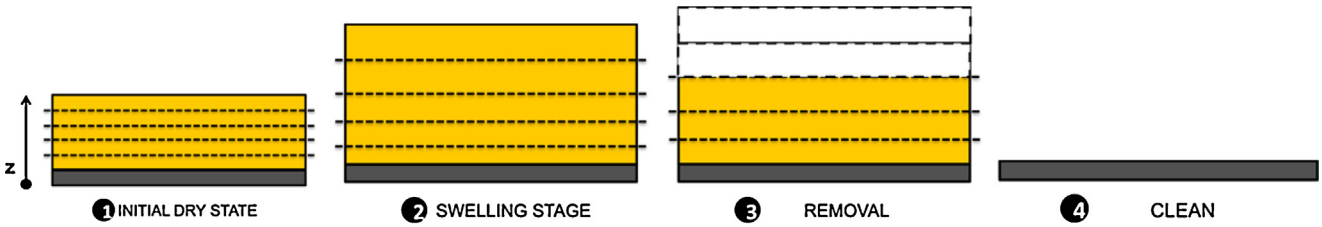

Fig. 10 – Schematic of the cleaning process. Removal of the layers occurs when the net removal calculated is higher than the thickness of one or more of the layers above. Yellow tone simulates the colour of egg yolk. (For interpretation of the references to color in figure legend, the reader is referred to the web version of the article.)

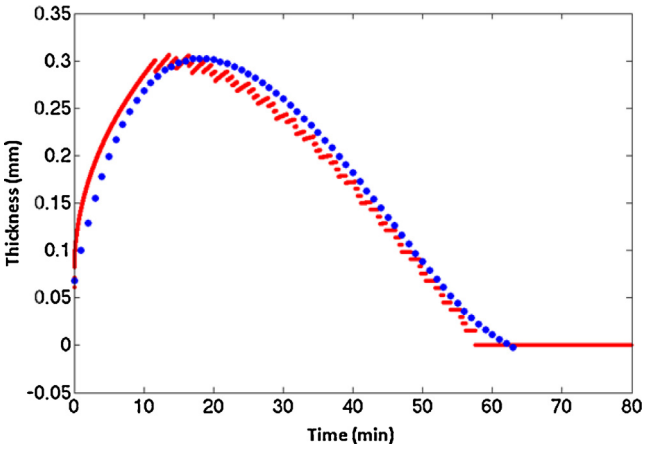

Fig. 11 – Simulation results versus real data. Blue colour represents experimental averaged fitted data. Red colour represents simulated data. Experimental conditions: 50 °C, pH 10.5, [Enzyme] = standard, shear stress = 24 Pa, frequency = 17%. 50 theoretical layers considered. (For interpretation of the references to color in figure legend, the reader is referred to the web version of the article.)

3.3.5. *Simulation example*

In Fig. 11, a simulation performed by the developed algorithm is compared to averaged fitted experimental data. This frequency corresponded to the analysis of three different points over the soil at intervals of a minute with a repetition pattern every 3 min. Experimental data was acquired approximately during 30 s per point as the rest of the time is spent on moving and placing the nozzle in the defined location. Table 2 summarises the parameters under which the simulation was run.

The plot shows how the algorithm is able to compute the observed swelling and removal. The removal of the layers is represented by each of the small 'jumps' that can be seen in the graph. Accordingly to what is seen in experimental data (see Fig. 3), swelling and removal mechanisms acting at similar rates are shown around the curve maximum. Anytime a layer is removed a decrease in thickness is seen. If no layer removal happens, the algorithm still computes for swelling and thickness increases.

The accuracy of the simulation could be improved by using a higher number of theoretical layers. This would lead to smoother curves and therefore higher sensitivity. However, the computational cost would be compromised. The higher the number of theoretical layers, the lower the time step and so, more calculations would be required to reach the solution. Fig. 12 represents the relationship between the quality of the simulation and the computational time as a function of the number of theoretical layers defined. Above 20 theoretical layers the computational time required to simulate the process increases exponentially while the quality of the prediction is not enhanced very much.

Table 2 – Values of the parameters used for simulation example.

Mechanisms	Parameter	Value
General specifications	Theoretical layers	50
	Time step, Δt(ms)	3
Swelling	Effective diffusion coefficient, D_{eff} (m^2/s)	2.5×10^{-10}
	Flory–Huggins parameter, χ	0.9
	Polymer chains per unit volume, N (chains/m^3)	$6. \times 10^{26}$
Removal	Shear stress removal rate, k_{ss} (μm/min)	25.10
	Soil dissolution removal rate, k_{ds} (μm/min)	5.55
	Lag time (min)	9

3.3.6. *Other outputs*

The algorithm also allows different information to be estimated. In Fig. 13, a series of possible outputs is shown. If the initial soil dry mass is known, a soil mass content can be assigned to each layer and the amount of soil remaining can be estimated as seen in Fig. 13A. The net amount of mass in the system (soil + solvent) can also be calculated when increase in thickness is correlated with the amount of solvent (water) uptake via a density relationship. This is seen in Fig. 13B. A cleaning percentage profile can be calculated if cleaning rate is normalised as a function of the layers remaining. This approach can lead to better comparison between cleaning rates for different systems. It establishes a common cleaning scale for different procedures and soil

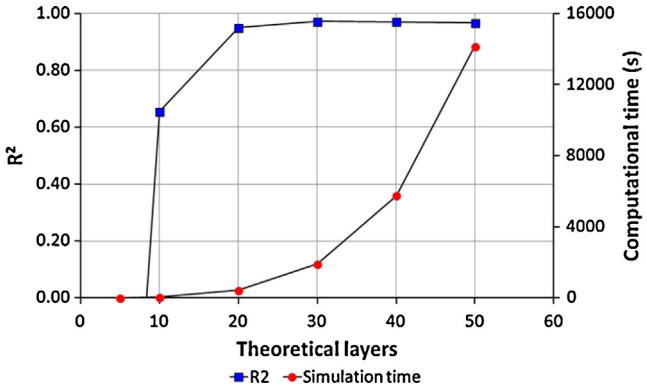

Fig. 12 – Computational cost (s) in CPU time, and quality of the analysis (R^2) as a function of number of theoretical layers defined.

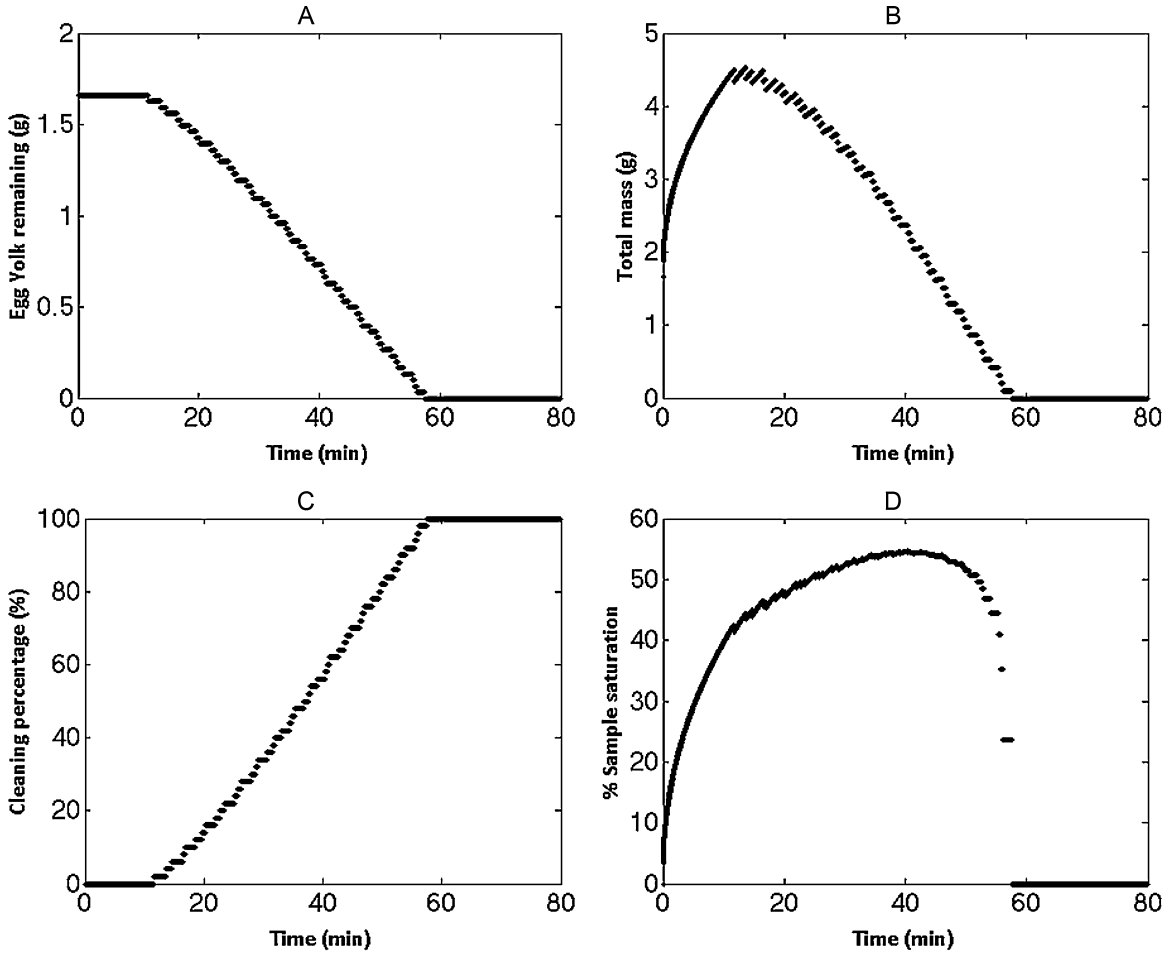

Fig. 13 – Other outputs that can be obtained with the algorithm developed. A – Soil remaining over time; B – total mass (soil + solvent) over time; C – cleaning percentage over time; D – sample saturation over time.

types as cleaning is evaluated in a scale from 0 to 100. The graph is shown in Fig. 13C. Finally, the increase of layers' thickness can be correlated with the equilibrium thickness and their 'saturation' calculated. 'Saturation' tells whether the soil network has 'room' for further swelling (or solvent uptake). Data calculated can be analysed for different numbers of layers (i.e. individual layers, group of bottom/top layers, all layers, etc.) depending on the information required. In Fig. 13D, the saturation of the soil is represented considering all the layers available at each time of the process. Maximum saturation is estimated around 50–60%. This indicates that if no removal happens, the soil still has the potential to hydrate by another 40%. At the end of the process, the routine predicts a decrease in the saturation of the remaining soil. This corresponds to the bottom layers, which are calculated theoretically to be low hydrated, as the liquid penetration is low. Once all layers are removed the curve drops to a 0% value.

4. Conclusions

The use of scanning fluid dynamic gauge (sFDG) has allowed the identification of the different mechanisms involved in a typical protein-based (egg yolk) cleaning process: swelling and removal via application of an external shear stress (mechanical and enzymatic-induced cleaning) or soil dissolution (pure enzymatic-induced cleaning). As a consequence, a novel algorithm has been developed to describe and model this behaviour. The process has been mathematically expressed in Eq. (1).

Swelling has been described through the use of combined mass transport and long deformation theories. The second order non-linear partial differential equation given has allowed the introduction of 'theoretical layers'. These theoretical layers correspond to the number of parts into which the initial dry thickness of the soil is divided. A mathematical requirement to comply with the convergence in the solution of the PDE includes as well the introduction of a time step. This has been used further on to integrate the removal mechanisms.

Cleaning phenomena have been modelled empirically. For each of the removal mechanisms identified (shear stress removal and soil dissolution), removal rates over time have been calculated by subtracting the positive contribution to thickness from swelling. Results have shown constant removal rates after an initial induction period with increasing removal rates. Different temperatures and frequencies of application of shear stress have been explored. An increase in temperature increased the removal rates observed for any of the cleaning mechanism involved. The constant application of shear stress over a fixed location promoted a reduction in the instantaneous cleaning rate observed. The hypothesis given is that there was an enzyme reaction rate limiting stage. Long intervals without the application of an external mechanical cleaning action allowed higher quantities of soil to be removed when mechanical action was applied. At 50 °C and with a

Please cite this article in press as: Pérez-Mohedano, R., et al., Development of a swelling-removal model for the scanning fluid dynamic gauge. Food Bioprod Process (2014), http://dx.doi.org/10.1016/j.fbp.2014.10.001

continuous application of shear stress, results also indicated a stronger mechanical removal. In the first stages of the cleaning process (induction period), removal rates were higher than for a discontinuous application of shear.

The algorithm developed is able to integrate all these phenomena. By using 'theoretical layers' and its associated time step, overall cleaning process has been modelled. The deletion of layer occurs over time if the accumulated removal thickness over a time step exceeds the thickness of the layer(s) above. The approach used also allows different ways of presenting the results. Cleaning can be expressed as thickness evolution over time, as a percentage, as the amount of soil left or total mass (soil + solvent) of the system at any time. A saturation analysis, expressed as the potential for further swelling, can also be performed.

Acknowledgements

This research was funded by the Engineering and Physical Sciences Research Council (EPSRC) and industrially sponsored by Procter&Gamble (P&G). The authors would like to thank Alam Zayeed, Carlos Amador and Ashmita Randhawa from Procter & Gamble and Chad VanderRoest and Blair Mikkelsen from Whirlpool Corporation for the support given during the realisation of this work.

References

Aehle, W., 2007. Enzymes in Industry: Production and Applications, third ed. Wiley-VCH Verlag GmbH & Co. KGaA, Weinheim, Germany, http://dx.doi.org/10.1002/9783527617098.

Biot, M.A., 1941. General theory of three dimensional consolidation. J. Appl. Phys. 12, 155–164.

Bird, M.R., Fryer, P.J., 1991. An experimental study of the cleaning of surfaces fouled by whey proteins. Food Bioprod. Process. Trans. Inst. Chem. Eng. C 69, 13–21.

Booth, D.T., 2003. Composition and energy density of eggs from two species of freshwater turtle with twofold ranges in egg size. Comp. Biochem. Physiol. A: Mol. Integr. Physiol. 134, 129–137, http://dx.doi.org/10.1016/S1095-6433(02)00216-7.

Bouklas, N., Huang, R., 2012. Swelling kinetics of polymer gels: comparison of linear and nonlinear theories. Soft Matter 8, 8194, http://dx.doi.org/10.1039/c2sm25467k.

Brazel, C.S., Peppas, N.A., 2000. Modeling of drug release from swellable polymers. Eur. J. Pharm. Biopharm. 49, 47–58, http://dx.doi.org/10.1016/S0939-6411(99)00058-2.

Chew, J.Y.M., Paterson, W.R., Wilson, D.I., Höufling, V., Augustin, W., 2005. A method for measuring the strength of scale deposits on heat transfer surfaces. Dev. Chem. Eng. Miner. Process. 13, 21–30, http://dx.doi.org/10.1002/apj.5500130103.

Denmat, M., Anton, M., Gandemer, G., 1999. Protein denaturation and emulsifying properties of plasma and granules of egg yolk as related to heat treatment. J. Food Sci. 64, 194–197, http://dx.doi.org/10.1111/j. 1365-2621.1999.tb15863.x.

Dürr, H., 2002. Milk heat exchanger cleaning: modelling of deposit removal II. Food Bioprod. Process. 80, 253–259, http://dx.doi.org/10.1205/096030802321154745.

Dürr, H., Graßhoff, A., 1999. Milk heat exchanger cleaning: modelling of deposit removal. Food Bioprod. Process. 77, 114–118, http://dx.doi.org/10.1205/096030899532402.

Flory, P.J., Rehner Jr., J., 1943. Statistical mechanics of cross-linked polymer networks II. Swelling. J. Chem. Phys. 11, 521–526.

Fryer, P.J., Asteriadou, K., 2009. A prototype cleaning map: a classification of industrial cleaning processes. Trends Food Sci. Technol. 20 (2009), 255–262, http://dx.doi.org/10.1016/j.tifs.2009.03.005.

Gibbs, J.W., 1906. The Scientific Papers of Willian Gibbs. http://books.google.com/books?id=-neYVEbAm4oC&oe=UTF-8 (accessed 12.09.13).

Gordon, P.W., Brooker, A.D.M., Chew, Y.M.J., Letzelter, N., York, D.W., Wilson, D.I., 2012. Elucidating enzyme-based cleaning of protein soils (gelatine and egg yolk) using a scanning fluid dynamic gauge. Chem. Eng. Res. Des. 90, 162–171, http://dx.doi.org/10.1016/j.cherd.2011.07.007.

Gordon, P.W., Brooker, A.D.M., Chew, Y.M.J., Wilson, D.I., York, D.W., 2010a. A scanning fluid dynamic gauging technique for probing surface layers. Meas. Sci. Technol. 21, 085103, http://dx.doi.org/10.1088/0957-0233/21/8/085103.

Gordon, P.W., Brooker, A.D.M., Chew, Y.M.J., Wilson, D.I., York, D.W., 2010b. Studies into the swelling of gelatine films using a scanning fluid dynamic gauge. Food Bioprod. Process. 88, 357–364, http://dx.doi.org/10.1016/j.fbp.2010.08.012.

Hong, W., Liu, Z., Suo, Z., 2009. Inhomogeneous swelling of a gel in equilibrium with a solvent and mechanical load. Int. J. Solids Struct. 46, 3282–3289, http://dx.doi.org/10.1016/j.ijsolstr.2009.04.022.

Hong, W., Zhao, X., Zhou, J., Suo, Z., 2008. A theory of coupled diffusion and large deformation in polymeric gels. J. Mech. Phys. Solids 56, 1779–1793, http://dx.doi.org/10.1016/j.jmps.2007.11.010.

Liu, W., Christian, G.K., Zhang, Z., Fryer, P.J., 2006. Direct measurement of the force required to disrupt and remove fouling deposits of whey protein concentrate. Int. Dairy J. 16, 164–172, http://dx.doi.org/10.1016/j.idairyj.2005.02.008.

Martin, R.B., 1998. Free energies and equilibria of peptide bond hydrolysis and formation. Biopolymers 45, 351–353, http://dx.doi.org/10.1002/(SICI)1097-0282(19980415)45:5<351::AID-BIP3>3.0.CO;2-K.

Mercadé-Prieto, R., Chen, X.D., 2006a. Dissolution of whey protein concentrate gels in alkali. AIChE J. 52, 792–803, http://dx.doi.org/10.1002/aic.10639.

Mercadé-Prieto, R., Falconer, R.J., Paterson, W.R., Wilson, D.I., 2006b. Probing the mechanisms limiting dissolution of whey protein gels during cleaning. Food Bioprod. Process. 84, 311–319, http://dx.doi.org/10.1205/fbp06021.

Mercadé-Prieto, R., Falconer, R.J., Paterson, W.R., Wilson, D.I., 2007a. Swelling and dissolution of beta-lactoglobulin gels in alkali. Biomacromolecules 8, 469–476, http://dx.doi.org/10.1021/bm060553n.

Mercadé-Prieto, R., Paterson, W.R., Dong Chen, X., Ian Wilson, D., 2008. Diffusion of NaOH into a protein gel. Chem. Eng. Sci. 63, 2763–2772, http://dx.doi.org/10.1016/j.ces.2008.02.029.

Mercadé-Prieto, R., Paterson, W.R., Wilson, D.I., 2007b. The pH threshold in the dissolution of beta-lactoglobulin gels and aggregates in alkali. Biomacromolecules 8, 1162–1170, http://dx.doi.org/10.1021/bm061100l.

Mercadé-Prieto, R., Paterson, W.R., Wilson, D.I., 2009. Effect of salts on the alkaline degradation of β-lactoglobulin gels and aggregates: existence of a dissolution threshold. Food Hydrocoll. 23, 1587–1595, http://dx.doi.org/10.1016/j.foodhyd.2008.11.007.

Mercadé-Prieto, R., Sahoo, P.K., Falconer, R.J., Paterson, W.R., Ian Wilson, D., 2007c. Polyelectrolyte screening effects on the dissolution of whey protein gels at high pH conditions. Food Hydrocoll. 21, 1275–1284, http://dx.doi.org/10.1016/j.foodhyd.2006.09.015.

Métais, A., Mariette, F., 2003. Determination of water self-diffusion coefficient in complex food products by low field 1H PFG-NMR: comparison between the standard spin-echo sequence and the T1-weighted spin-echo sequence. J. Magn. Reson. 165, 265–275, http://dx.doi.org/10.1016/j.jmr.2003.09.001.

Mine, Y., Zhang, H., 2013. Biochemistry of foods. In: Biochemistry of Foods, third ed. Elsevier, http://dx.doi.org/10.1016/B978-0-08-091809-9. 00005-4.

Oztop, M.H., McCarthy, K.L., 2011. Mathematical modeling of swelling in high moisture whey protein gels. J. Food Eng. 106, 53–59, http://dx.doi.org/10.1016/j.jfoodeng.2011.04.007.

Peppas, N.A., Brannon-Peppas, L., 1994. Water diffusion and sorption in amorphous macromolecular systems and foods. J. Food Eng. 22, 189–210, http://dx.doi.org/10.1016/0260-8774(94)90030-2.

Please cite this article in press as: Pérez-Mohedano, R., et al., Development of a swelling-removal model for the scanning fluid dynamic gauge. Food Bioprod Process (2014), http://dx.doi.org/10.1016/j.fbp.2014.10.001

Peppas, N.A., Sinclair, J.L., 1983. Anomalous transport of penetrants in glassy polymers. Colloid Polym. Sci. 261, 404–409.

Saikhwan, P., Mercadé-Prieto, R., Chew, Y.M.J., Gunasekaran, S., Paterson, W.R., Wilson, D.I., 2010. Swelling and dissolution in cleaning of whey protein gels. Food Bioprod. Process. 88, 375–383, http://dx.doi.org/10.1016/j.fbp.2010.09.006.

Tsutsui, T., 1988. Functional properties of heat-treated egg yolk low density lipoprotein. J. Food Sci. 53, 1103–1106.

Tuladhar, T., Paterson, W.R., Macleod, N., Wilson, D.I., 2000. Development of a novel non-contact proximity gauge for thickness measurement of soft deposits and its application in fouling studies. Can. J. Chem. Eng. 78, 935–947, http://dx.doi.org/10.1002/cjce.5450780511.

Tuladhar, T.R., Paterson, W.R., Wilson, D.I., 2002. Thermal conductivity of whey protein films undergoing swelling. Food Bioprod. Process. 80, 332–339, http://dx.doi.org/10.1205/096030802321154862.

Wilson, D.I., 2005. Challenges in cleaning: recent developments and future prospects. Heat Transf. Eng. 26, 51–59, http://dx.doi.org/10.1080/01457630590890175.

Xin, H., Chen, X.D., Özkan, N., 2004. Removal of a model protein foulant from metal surfaces. AIChE J. 50, 1961–1973, http://dx.doi.org/10.1002/aic.10149.

Please cite this article in press as: Pérez-Mohedano, R., et al., Development of a swelling-removal model for the scanning fluid dynamic gauge. Food Bioprod Process (2014), http://dx.doi.org/10.1016/j.fbp.2014.10.001